Online Detection and SNR Estimation in Cooperative Spectrum Sensing

Jesus Perez, Javier Via, Luis Vielva, and David Ramírez, *Senior Member, IEEE*

***Abstract*— Cooperative spectrum sensing has proved to be an effective method to improve the detection performance in cognitive radio systems. This work focuses on centralized cooperative schemes based on the soft fusion of the energy measurements at the cognitive radios (CRs). In these systems, the likelihood ratio test (LRT) is the optimal detection rule, but the sufficient statistic depends on the local signal-to-noise ratio (SNR) at the CRs, which are unknown in most practical cases. Therefore, the detection problem becomes a composite hypothesis test. The generalized LRT is the most popular approach in those cases. Unfortunately, in mobile environments, its performance is well below the LRT because the local energies are measured under varying SNRs. In this work, we present a new algorithm that jointly estimates the instantaneous SNRs and detects the presence of primary signals. Due to its adaptive nature, the algorithm is well suited for mobile scenarios where the local SNRs are time-varying. Simulation results show that its detection performance is close to the LRT in realistic conditions.**

***Index Terms*— Cooperative spectrum sensing, energy detection, expectation-maximization (EM) algorithm, maximum likelihood, probabilistic mixture models.**

I. Introduction

SPECTRUM sensing is a key operation in cognitive radio. Through spectrum sensing the cognitive radios (CRs) aim at detecting frequency bands that are not being used by the primary network. The performance of spectrum sensing is limited by shadowing and multi-path effects in the channels between the primary users (PUs) and the CRs (sensing channels). By using cooperative spectrum sensing (CSS) the impact of those effects can be mitigated efficiently by the inherent multiuser/spatial diversity of the CR network [1]–[3]. In centralized CSS, the CRs individually perform local sensing and report their sensing output to a fusion center (FC) through a dedicated control channel. Then, the FC combines the information received from the CRs to make a decision on the presence of primary signals in the given frequency band.

This work considers CSS based on the soft combination of the energy levels measured by single antenna CRs. Unlike other detection techniques, energy detection does not require prior knowledge of PU signals characteristics. This fact, together with its simplicity and general applicability, makes energy detection the most popular technique in CSS [1]–[5].

A well-known alternative to soft combining is the so-called hard combining scheme, where each CR makes its own decision, according to the local energy measurements, and reports it to the FC. Then, the FC makes the final decision combining the CRs decisions. In general, soft fusion achieves better detection performance. Even equal-gain combining (EGC), the combining scheme that simply adds the local energy measurements [6], outperforms hard fusion in most cases [7]. The EGC detector is also called sum-fusion detector in the technical literature [8]. Quantized soft combining has been proposed as a compromise between soft and hard fusion [7], [9]–[11]. In this case, the CRs report quantized measurements of the energy to the FC.

In soft energy fusion, the likelihood ratio test (LRT) is optimal when the FC knows the instantaneous signal-to-noise ratio (SNR) at the CRs [12], [13]. The LRT sufficient statistic is a linear combination of the measured energy levels at the CRs, where the coefficients are functions of the local SNRs [3], [4], [7], [14]. This is a major drawback because the FC needs to know the SNRs to apply the LRT, which are unknown in most practical cases. EGC does not require this SNR knowledge, but it performs significantly worse than the LRT, especially in low SNR scenarios [7]. Moreover, conventional SNR estimation methods are unfeasible in the spectrum sensing context because it is unknown when the primary signals are present in the channel. This is a vicious circle; the detection test requires estimating the SNRs and estimating the SNRs requires knowing whether the primary signals are present or absent. This problem becomes even more critical when the PU activity pattern is highly dynamic with short idle and busy periods. Since the SNRs are unknown, the detection problem becomes a composite hypothesis test [12], [13]. The generalized LRT (GLRT) is the most popular approach in those cases. In the GLRT, the SNRs values in the LRT are replaced by their maximum likelihood estimates (MLE) under the assumption that the primary signals are present in the channel. But in mobile environments, the local SNRs change between consecutive energy measurements, so, in principle, their MLE should be computed only from the current one.

Manuscript received March 3, 2021; revised July 23, 2021; accepted September 10, 2021. Date of publication September 23, 2021; date of current version April 11, 2022. This work was supported in part by the Ministerio de Ciencia, Innovación y Universidades, jointly with European Commission [European Regional Development Fund (ERDF)], under Grant TEC2017-86921-C2-1-R and Grant TEC2017-86921-C2-2-R (CAIMAN) and in part by The Comunidad de Madrid under Grant Y2018/TCS-4705 (PRACTICO-CM). The associate editor coordinating the review of this article and approving it for publication was D. Lopez-Perez. *(Corresponding author: Jesus Perez.)*

Jesus Perez, Javier Via, and Luis Vielva are with the Department of Communications Engineering, Universidad de Cantabria, 39005 Santander, Spain (e-mail: jesus.perez@unican.es).

David Ramírez is with the Department of Signal Theory and Communications, Universidad Carlos III de Madrid, 28915 Leganés, Spain, and also with Gregorio Marañón Health Research Institute, 28007 Madrid, Spain (e-mail: david.ramirez@uc3m.es).

Color versions of one or more figures in this article are available at https://doi.org/10.1109/TWC.2021.3113089.

Digital Object Identifier 10.1109/TWC.2021.3113089

This leads to poor estimates of the instantaneous SNRs, which results into a GLRT performance well below that of the LRT.

A common way to circumvent the estimation of the instantaneous SNRs is to assume a specific distribution of the sensing channels with unknown parameters, which are easier to estimate than the instantaneous SNRs. Also, the channels' responses at different times are assumed to be independent. Following this approach, different soft fusion detectors have been proposed [8], [15]–[17]. Those detectors are suited for the assumed channel distribution, but they lack the ability to adapt to a changing environment with arbitrary time-correlated channels.

In [18], the authors combined batch algorithms with time-sliding windows to sequentially estimate the local SNRs from the energy measurements. The drawback is that the energy measurements in the sliding window have the same weight in the SNRs estimates, regardless of when they were measured. The decision threshold setting was not addressed.

Also related to the present work is [19], where a cooperative sequential detection scheme, based on the sequential probability ratio test (SPRT) [20], is presented. The CRs report their local log-likelihood ratio (LLR) of every acquired sample, and the FC sequentially accumulates the log-likelihood statistics and performs the SPRT. The authors present a method to implement the scheme when the signal models have unknown parameters. This approach to CSS is quite different from ours. Due to the SPRT nature, the goal is to minimize the number of signal samples before making the decision subject to constraints on the probability of false alarm and missed detection. Moreover, the CRs must report the LLR of every acquired sample to the FC. Also based on the SPRT, [21] proposes a decentralized cooperative detection scheme where the CRs do not report their LLRs in parallel to the FC, but they do it sequentially.

The SNR estimation in the spectrum sensing context has been addressed considering multi-antenna settings [22], and fractional-sampling [23]. Although from a signal processing point of view, these schemes are equivalent to a cooperative system, the fundamental difference is the information available to estimate the SNR. In those schemes, the SNR is estimated by a single CR from all signal samples. In our case, is the FC who estimates the SNRs from the energy measurements at the CRs.

Contribution: In this work, we propose a novel approach to CSS based on a probabilistic mixture model [24], [25] of the energy measurements. The model has two components associated with the presence or absence of primary signals. The energy measurements are observed variables, the channel occupancy is a latent (hidden) variable, and the instantaneous SNRs are unknown model parameters. From this model, we derive an online algorithm that jointly estimates the instantaneous SNRs and detects the presence of primary signals from the local energy measurements at the CRs. It is an online classification EM (expectation-maximization) algorithm [26]–[28]. We derive simple closed-form expressions for both the E-step and the M-step taking into account the exact distribution of the energy measurements.

In realistic scenarios, the sensing channels, and thus the SNRs, change slowly between consecutive sensing periods. Then, the estimates of the SNRs can be improved taking into account not only the current energy measurements but also previous ones. The algorithm does that by implicitly assigning different weights to the energy observations according to the time when they were measured. In the extreme case of considering only the last energy measurements, the algorithm reduces to the one-shot GLRT. The proposed algorithm works well for any PU activity pattern, even when it exhibits short busy and idle periods. Simulation results show that its estimation performance is excellent in practical cases, so its detection performance is close to that of the LRT detector. In most realistic scenarios, the proposed method clearly outperforms the one-shot GLRT.

The algorithm is fully blind, that is, the only input is the energy measurements from the sensors. It is computationally simple, and the processing of each energy measurement takes a fixed time. The energy measurements are processed sequentially in time so it does not need to store them. Therefore, the proposed method requires very little (and constant) memory use. Since it adapts to the instantaneous SNRs, the proposed detector is valid for any distribution of the sensing channels, even when they are different for each CR. To the best of our knowledge, no online detection algorithm with the above characteristics has been proposed in the context of energy spectrum sensing. The fact that the detection algorithm also estimates the instantaneous SNRs is a distinct feature that differentiates it from other existing CSS detectors.

We also propose a new method to approximate the distribution of the test statistic of the LRT and of the proposed detector. It is a moment-matching method [29], [30], which tightly approximates, under both hypotheses, the distributions of the test statistic by Gamma distributions with properly selected parameters. These depend on the cumulants of the true distribution, which can be calculated in closed form for the null (idle) hypothesis, and only depending on the SNRs for the alternative (busy) hypothesis. Thus, we can accurately set the decision threshold for a prescribed probability of false alarm at each time.

Notation: Throughout this paper we use bold-face letters for vectors and light-face letters for scalar quantities. The superscript $\mathbf{x}^T$ refers to the transpose of $\mathbf{x}$. x^+ denotes $\max\{x, 0\}$ and $\hat{\theta}$ refers to the estimate of parameter θ. $X \sim CN(\mu,\ \sigma^2)$ indicates that X is a complex circular Gaussian random variable with mean μ and variance σ^2, and $X \sim \chi^2_k$ indicates that X is a chi-squared random variable with k degrees of freedom. Finally, $\mathbb{E}[X]$ denotes the expectation of the random variable X.

Paper Organization: The remainder of this paper is organized as follows. Section II describes the system model and derives the true distribution of the energy measurements. Afterwards, Section III derives the cooperative LRT, the one-shot GLRT and the EGC detector. The proposed algorithm is presented in Section IV. Section V addresses the derivation of the decision thresholds for the aforementioned detectors. Section VI presents simulations results that show the estimation and detection performance of the proposed

algorithm and compare it with those of the other methods. Finally, Section VII concludes the paper.

II. System Model

We consider a single PU operating in a given frequency channel. Let $s \in \{0,1\}$ indicate the state of the PU, where $s=1$ when it is transmitting and $s=0$ when it is not.

A. Energy Estimates

Let us consider a sensing network with J cooperative CRs. The m-th baseband complex signal sample at CR j is

$$\begin{aligned} \mathcal{H}_0 &: z_j(m) = r_j(m), \\ \mathcal{H}_1 &: z_j(m) = h_j\ y(m) + r_j(m), \end{aligned} \tag{1}$$

where $\mathcal{H}_0$ and $\mathcal{H}_1$ denote the hypotheses $s=0$ and $s=1$, respectively, $y(m)$ is the signal transmitted by the PU, h_j denotes the complex channel gain from the PU to the CR j, and $r_j(m)$ is the noise at the CR j. The noise is assumed to be a zero-mean, white, complex circular Gaussian process with variance σ_j^2. We also model $y(m)$ as zero-mean circular complex Gaussian process, which is particularly accurate if the PU transmits multi-carrier modulated signals. This is a standard assumption in the spectral sensing literature [5], [7], [14]. Even if this is not the case, the Gaussian model leads to tractable analysis and useful detectors. Since $r_j(m)$ and $y(m)$ are independent, we have

$$\mathcal{H}_s : z_j(m) \sim CN(0,\ \sigma_j^2 + s\ P\ |h_j|^2), \quad s=0,1, \tag{2}$$

where P denotes the variance of $y(m)$.

The normalized energy estimate at CR j is [4]

$$e_j = \frac{1}{\sigma_j^2} \sum_{m=1}^{M} |z_j(m)|^2, \tag{3}$$

where M is the number of signal samples used to estimate the energy. We assume that the PU state does not change during the sensing time interval when the signal samples are acquired. This requires M to be relatively small. Notice that, to compute the normalized energy (3), each CR has to know its noise power, which is a common assumption in the CSS literature [3], [5], [7], [11], [14], [16], [17], [31].

B. Distribution of the Energy Estimates

Considering (2) and (3), the energy estimates are random variables with the following distribution [32],

$$\mathcal{H}_s : e_j = \frac{1+s\ g_j}{2}\ X_j, \quad s=0,1, \tag{4}$$

where $X_j \sim \chi^2_{2M}$ and $g_j = P\ |h_j|^2/\sigma_j^2$ is the SNR at CR j when the PU is active.

According to (4), the probability density function (pdf) of e_j, conditioned to s and g_j, is

$$f(e_j|s,g_j) = \frac{e_j^{M-1}}{\Gamma(M)(1+s\ g_j)^M} \exp\left(\frac{-e_j}{1+s\ g_j}\right). \tag{5}$$

Notice that when $s=0$ the pdf does not depends on g_j.

Let $\mathbf{e} = [e_1 \dots e_J]^T$ be the vector whose entries are the energy estimates at the CRs. Assuming that they are independent (for a given s), the pdf of the energy vector will be

$$f(\mathbf{e}|s,\mathbf{g}) = \prod_{j=1}^{J} f(e_j|s,g_j), \tag{6}$$

where $\mathbf{g} = [g_1 \dots g_J]^T$ denotes the SNRs vector. Strictly speaking, the energy estimates at different CRs are not conditionally independent under $\mathcal{H}_1$ because they depend somehow on the signal transmitted by the PU (see (1)). In any case, in the low and medium SNR regime, they can be considered independent because the noise at the CRs are independent and the sensing channels are different. Independence of the energy measurements is a common assumption in the technical literature [1], [7], [14].

III. Cooperative Detectors

After each local measurement, the CRs report the energy values (3) to the FC through the control channels, which are assumed to be error-free. Once the measurements are available at the FC, it decides on the presence of primary signals on the channel.

A. LRT Detector

Assuming that the SNRs are known at the FC, the optimal detector is the LRT [13]:

$$\frac{f(\mathbf{e}|\mathcal{H}_1)}{f(\mathbf{e}|\mathcal{H}_0)} = \frac{f(\mathbf{e}|s=1,\mathbf{g})}{f(\mathbf{e}|s=0,\mathbf{g})} \underset{\mathcal{H}_0}{\overset{\mathcal{H}_1}{\gtrless}} \gamma_0. \tag{7}$$

Considering (5) and (6), and taking logarithms, (7) can be written as follows

$$\sum_{j=1}^{J} e_j\ \frac{g_j}{1+g_j} \underset{\mathcal{H}_0}{\overset{\mathcal{H}_1}{\gtrless}} \gamma_{LRT}, \tag{8}$$

where $\gamma_{LRT} = \log\gamma_0 + M\sum_{j=1}^{J}\log(1+g_j)$. Notice that this test statistic depends on the SNRs.

B. EGC Detector

The EGC, also called sum fusion detector, is the suboptimal detector that simply adds up the energy measurements,

$$\sum_{j=1}^{J} e_j \underset{\mathcal{H}_0}{\overset{\mathcal{H}_1}{\gtrless}} \gamma_{EGC}. \tag{9}$$

It does not require the FC to know the SNRs, but its detection performance is typically poor when the SNRs are low. On the other hand, we must point out that the EGC detector tends to the LRT in the high SNR region, $g_j \gg 1$.

C. One-Shot GLRT Detector

When the primary SNRs are unknown, the problem becomes a composite hypothesis test. The most popular approach to these problems is the GLRT [13], where the unknown parameters of the LRT are replaced by their MLE under

both hypotheses. Then, taking into account that there are no unknown parameters under H_0, the GLRT becomes

$$\sum_{j=1}^{J} e_j \ \frac{\hat{g}_j}{1+\hat{g}_j} \underset{\mathcal{H}_0}{\overset{\mathcal{H}_1}{\gtrless}} \gamma_{GLRT}, \tag{10}$$

where $\hat{g}_j$ denotes the ML estimate of g_j, from e_j, assuming $s=1$, and is given by

$$\hat{g}_j = \underset{g_j \geq 0}{\operatorname{argmax}} \ f(e_j|s=1,g_j).$$

Appendix A shows that

$$\hat{g}_j = \frac{1}{M}\left(e_j - M\right)^+. \tag{11}$$

From (4), the mean of e_j under the null hypothesis is M. Therefore, apart from the factor $1/M$, the estimate $\hat{g}_j$ is the deviation of e_j from its mean under $\mathcal{H}_0$.

Substituting (11) into (10), after some algebraic manipulations (see appendix B), the one-shot GLRT reduces to

$$\sum_{j=1}^{J}(e_j - M)^+ \underset{\mathcal{H}_0}{\overset{\mathcal{H}_1}{\gtrless}} \gamma_{GLRT}. \tag{12}$$

Unfortunately, the performance of this detector is poor since the estimates $\hat{g}_j$ are typically inaccurate. Notice that the number of parameters to estimate (J) equals the number of observations, and each parameter (g_j) is estimated from a single observation (e_j). Also, M is typically small, so the energy estimates are inaccurate. Moreover, the one-shot GLRT lacks the ability to learn from past observations.

IV. EM-Based Detector

In many practical cases, the coherence time of the sensing channels is of the order of the time elapsed between consecutive sensing periods. In those cases, $\mathbf{g}$ exhibits a significant correlation at consecutive sensing periods. Then, $\mathbf{g}$ could be better estimated by considering multiple energy measurements rather than a single one, as in the one-shot GLRT. This is the basis of the detector proposed in this section.

From (5) and (6), marginalizing out s, the pdf of the energy vectors is

$$f(\mathbf{e}|\mathbf{g}) = \alpha_0 \ f(\mathbf{e}|s=0) + \alpha_1 \ f(\mathbf{e}|s=1,\mathbf{g}), \tag{13}$$

where α_1 and $\alpha_0 = 1-\alpha_1$ are the prior probabilities of $s=1$ and $s=0$, respectively. In the spectrum sensing context, α_1 is known as the channel occupancy rate (COR), which is assumed to be known by the FC. The COR estimation has been an active research area in the last years, and a variety of algorithms have been proposed [33]–[37]. The marginal distribution, (13), can be viewed as a mixture model [24], [25] with two components, $f(\mathbf{e}|s=0)$ and $f(\mathbf{e}|s=1,\mathbf{g})$, being α_0 and α_1 the mixing coefficients. The energy measurements, $\mathbf{e}$, are observed (visible) variables, the PU state, s, is a latent (hidden) variable, and the SNRs, $\mathbf{g}$, are the unknown model parameters.

A. Online EM Algorithm

The expectation-maximization (EM) algorithm [38] is the most popular method for ML estimation in mixture models with latent variables. Since the energy measurements arrive at the FC sequentially, we focus on sequential EM methods, being the most popular one the so-called Stepwise EM (SEM), [25], [27], [28]. As we will see later, this algorithm is very well suited to our problem because it leads to simple closed-form expressions. Let $\mathbf{x}$ denotes the observed variables and $\mathbf{y}$ the latent variables. The pair $\{\mathbf{x},\mathbf{y}\}$ is called the complete-data. Given $\{\mathbf{x},\mathbf{y}\}$, the SEM algorithm assumes that the complete-data likelihood belongs to the exponential family,

$$L_c(\boldsymbol{\theta}) = h(\mathbf{x},\mathbf{y}) \ \exp\left(\boldsymbol{\eta}(\boldsymbol{\theta})^T \boldsymbol{\Phi}(\mathbf{x},\mathbf{y})\right)/z(\boldsymbol{\theta}), \tag{14}$$

where $\boldsymbol{\theta}$ denotes the set of unknown model parameters. The terms $h(\mathbf{x},\mathbf{y}), \boldsymbol{\eta}(\boldsymbol{\theta}), \boldsymbol{\Phi}(\mathbf{x},\mathbf{y})$, and $z(\boldsymbol{\theta})$ are called scaling function, parameters function, sufficient statistic and partition function, respectively.

According to the SEM algorithm, each time a new observation $\mathbf{x}_n$ is available, the estimate of the parameters is updated as follows,

$$\hat{\boldsymbol{\theta}}_n = \underset{\boldsymbol{\theta}}{\operatorname{argmax}} \ \boldsymbol{\eta}(\boldsymbol{\theta})^T \boldsymbol{\phi}_n - \log z(\boldsymbol{\theta}), \tag{15}$$

where

$$\boldsymbol{\phi}_n = (1-\mu_n)\boldsymbol{\phi}_{n-1} + \mu_n \ \mathbb{E}\left[\boldsymbol{\Phi}(\mathbf{x}_n,\mathbf{y}_n)|\mathbf{x}_n,\hat{\boldsymbol{\theta}}_{n-1}\right]. \tag{16}$$

The parameter $\mu_n \in (0,1)$ is the forgetting factor (also called learning rate or stepsize) at time n. Different stepsize sequences $\{\mu_n\}$ have been proposed for stationary scenarios [25], [27], [28] where the unknown parameters $\boldsymbol{\theta}$ do not change. In non-stationary scenarios, where the model parameters $\boldsymbol{\theta}$ are time-varying, a constant forgetting factor $\mu_n = \mu$ is typically used. The latter is our case because the sensing channels are time-varying. The SEM algorithm runs a single iteration each time a new observation $\mathbf{x}_n$ is available. Each iteration comprises two steps: the computation of the conditional expectation in (16), and the maximization in (15). They are the so-called E-step and M-step, which give the name to the algorithm. The E-step is aimed at incorporating the information that is brought by $\mathbf{x}_n$, and the M-step is a maximization program whose result is the update of the parameters estimate $\hat{\boldsymbol{\theta}}_n$.

For the problem at hand, the model parameters are the SNR at the CRs ($\mathbf{g}$), the observed variables are the energy measurements ($\mathbf{e}$), and the only latent variable is the PU state (s). Appendix C shows that, given $\mathbf{e}$ and s, the complete-data likelihood in our problem, $L_c(\mathbf{g})$, can be written in the exponential form (14) where the vector of sufficient statistic, the partition function and the parameters function are, respectively

$$\boldsymbol{\Phi}(\mathbf{e},s) = \begin{pmatrix} s \\ s\cdot\mathbf{e} \end{pmatrix}, \quad z(\mathbf{g}) = 1,$$
$$\boldsymbol{\eta}(\mathbf{g}) = -\begin{pmatrix} M\sum_{j=1}^{J}\log(1+g_j) \\ (1+g_1)^{-1} \\ \vdots \\ (1+g_J)^{-1} \end{pmatrix}. \tag{17}$$

The scaling term $h(\mathbf{e}, s)$ (see (39) in Appendix C) does not play any role in the algorithm.

Let $\mathbf{e}_n, s_n, \mathbf{g}_n$ denote the observed energy vector, the PU state, and the SNR vector at sensing period n, respectively. According to (15) and (16), each time a new energy vector $\mathbf{e}_n$ is observed, the current SNR vector is estimated as follows,

$$\hat{\mathbf{g}}_n = \underset{\mathbf{g}\geq\mathbf{0}}{\operatorname{argmax}}\ \boldsymbol{\eta}(\mathbf{g})^T \boldsymbol{\phi}_n, \tag{18}$$

where

$$\boldsymbol{\phi}_n = (1-\mu)\boldsymbol{\phi}_{n-1} + \mu\ \mathbb{E}\left[\boldsymbol{\Phi}(\mathbf{e}_n, s_n)|\mathbf{e}_n, \hat{\mathbf{g}}_{n-1}\right]. \tag{19}$$

Since the channels change over time, so do the SNRs. Therefore, we consider a constant forgetting factor, μ, whose value must be selected according to how fast the SNRs change between consecutive energy measurements.

Appendices D and E derive the following closed-form expressions for the E-step (19) and the M-step (18):

- E-step:

$$\boldsymbol{\phi}_n = \left[\ b_n\ \mathbf{a}_n^T\ \right]^T,$$

where

$$\begin{aligned} b_n &= (1-\mu)\ b_{n-1} + \mu\ \tilde{s}_n, \\ \mathbf{a}_n &= (1-\mu)\ \mathbf{a}_{n-1} + \mu\ \tilde{s}_n\ \mathbf{e}_n. \end{aligned} \tag{20}$$

The term $\tilde{s}_n = P(s_n = 1|\mathbf{e}_n, \hat{\mathbf{g}}_{n-1})$ is the probability that the PU was active when $\mathbf{e}_n$ was observed, given the last estimate $\hat{\mathbf{g}}_{n-1}$. Notice that $\tilde{s}_n$ can be considered as a soft estimate of s_n. In the context of the EM algorithm, $\tilde{s}_n$ is usually called the responsibility that $s_n = 1$ for observation $\mathbf{e}_n$. In our case, it is given by

$$\tilde{s}_n = \frac{1}{1+\frac{\alpha_0}{\alpha_1}\prod_{j=1}^{J}(1+\hat{g}_{n-1,j})^M \exp\left(-\frac{e_{n,j}\ \hat{g}_{n-1,j}}{1+\hat{g}_{n-1,j}}\right)}. \tag{21}$$

- M-step:

$$\hat{g}_{n,j} = \frac{1}{M}\left(\frac{a_{n,j}}{b_n} - M\right)^+, \quad j = 1, \ldots, J. \tag{22}$$

Interestingly, when $\mu = 1$, (22) reduces to the one-shot ML estimates used in the GLRT (11).

Initialization: We propose to initialize the algorithm to $\mathbf{a}_0 = \mathbf{0}, b_0 = 0$. Then, from (20) and (22), the first estimate of the SNRs reduces to the one-shot ML estimate (11) employed in the GLRT, that is

$$\hat{g}_{1,j} = \frac{1}{M}\left(e_{1,j} - M\right)^+, \quad j = 1, \ldots, J, \tag{23}$$

regardless the value of μ and $\tilde{s}_1$, as they cancel out in (22).

Interpretation: Assuming that the algorithm is initialized as above, the terms b_n and $\mathbf{a}_n$ can be written as follows

$$\begin{aligned} b_n &= \sum_{i=1}^{n} \mu\ (1-\mu)^{n-i}\ \tilde{s}_i, \\ \mathbf{a}_n &= \sum_{i=1}^{n} \mu\ (1-\mu)^{n-i}\ \tilde{s}_i\ \mathbf{e}_i. \end{aligned} \tag{24}$$

Then, substituting (24) into (22), the SNR estimates can be written as follows

$$\hat{g}_{n,j} = \frac{\left(\sum_{i=1}^{n}(1-\mu)^{n-i}\ \tilde{s}_i\ (e_{i,j} - M)\right)^+}{M\sum_{i=1}^{n}(1-\mu)^{n-i}\ \tilde{s}_i}. \tag{25}$$

This shows that the contribution of a given energy observation, $e_{i,j}$, to the SNR estimate $\hat{g}_{n,j}$ depends on its responsibility, $\tilde{s}_i$, and on the time when it was observed (i through the term $(1-\mu)^{n-i}$).

- When μ is close to 1 the algorithm tends to be memoryless. It forgets previous energy observations, so the SNR is mainly estimated from the last one ($e_{n,j}$). Moreover, the dominant term in (25) corresponds to $i = n$, so the SNR estimate tends to the one-shot ML estimate (11),

$$\hat{g}_{n,j} \xrightarrow{\mu\to 1} \frac{1}{M}\left(e_{n,j} - M\right)^+. \tag{26}$$

Therefore, apart from the factor $1/M$, the SNR estimate $\hat{g}_{n,j}$ is the deviation of $e_{n,j}$ from its mean value under the null hypothesis (M).

- On the other hand, when μ tends to zero, we have

$$\hat{g}_{n,j} \xrightarrow{\mu\to 0} \frac{1}{M}\left(\frac{\sum_{i=1}^{n}\tilde{s}_i\ (e_{i,j} - M)}{\sum_{i=1}^{n}\tilde{s}_i}\right)^+. \tag{27}$$

Now, factor $1/M$ aside, the SNR estimate is the weighted average of all energy deviations, where the weights are the responsibilities. Therefore, $\hat{g}_{n,j}$ averages the effective energy deviations at the times the PU is estimated to have been active.

B. Decision Rule

The responsibility (21) is an estimate of the probability that the PU was active when $\mathbf{e}_n$ was observed. It can be used to decide on the PU state [26]. Using Bayes' theorem,

$$\tilde{s}_n = P(s_n = 1|\mathbf{e}_n, \hat{\mathbf{g}}_{n-1}) = \frac{f(\mathbf{e}_n|s_n = 1, \hat{g}_{n-1})\ \alpha_1}{f(\mathbf{e}_n|\hat{g}_{n-1})}.$$

Similarly, the probability that the PU was inactive when $\mathbf{e}_n$ was observed is

$$1 - \tilde{s}_n = P(s_n = 0|\mathbf{e}_n, \hat{\mathbf{g}}_{n-1}) = \frac{f(\mathbf{e}_n|s_n = 0, \hat{g}_{n-1})\ \alpha_0}{f(\mathbf{e}_n|\hat{g}_{n-1})}.$$

Then, the decision rule can be expressed as a function of the responsibility as follows

$$\frac{f(\mathbf{e}_n|s_n = 1, \hat{\mathbf{g}}_{n-1})}{f(\mathbf{e}_n|s_n = 0, \hat{\mathbf{g}}_{n-1})} = \frac{\tilde{s}_n\ \alpha_0}{(1-\tilde{s}_n)\ \alpha_1} \underset{\mathcal{H}_0}{\overset{\mathcal{H}_1}{\gtrless}} \gamma_0. \tag{28}$$

Substituting the expression of the responsibility (21) into (28), after simple algebraic manipulations, the detection rule reduces to

$$\sum_{j=1}^{J} e_{n,j}\ \frac{\hat{g}_{n-1,j}}{1+\hat{g}_{n-1,j}} \underset{\mathcal{H}_0}{\overset{\mathcal{H}_1}{\gtrless}} \gamma_{EM}, \tag{29}$$

where $\gamma_{EM} = \log\gamma_0 + M\sum_{j=1}^{J}\log(1+\hat{g}_{n-1,j})$. Notice that the detection rule has the same form as in the LRT (8), but

using the SNR estimates at the time the energy vector is observed. Hereafter, we will refer to (29) as the EM detector.

Notice that the test statistic in (28) is a monotonic transformation of the responsibility, so $\tilde{s}_n$ might be used as the test statistic. Also, (29) allows us to compute the decision threshold, in a similar way as in the LRT. This will be shown in section V.

C. The Algorithm

In summary, each time the CRs report a new energy vector, the FC first applies the decision rule. Then it updates the SNRs estimate as it is shown in Algorithm 1. It is done in two steps: the computation of the responsibility (E-step), and the update of the SNRs estimate (M-step).

Algorithm 1 : EM Detection-Estimation

Input: J, M, μ
First energy measurements: $\mathbf{e}_1$
Compute $\hat{\mathbf{g}}_1$ from (23)
Repeat for each energy measurement $\mathbf{e}_n$, $n > 1$
  Decision on the channel occupancy from (29)
  E-step:
    - Compute $\tilde{s}_n$ from (21)
    - Compute $\mathbf{a}_n$ and b_n from (20)
  M-step:
    - Update $\hat{\mathbf{g}}_n$ from (22)

From a practical perspective, it is worth noting that each iteration takes fixed time and requires constant memory use.

V. Decision Thresholds

To set the decision threshold we first analyze the distribution of the test statistic of the detectors under the null hypothesis. Afterwards, we describe how to set the decision thresholds for a fixed false alarm probability, which is the most common criterion in spectrum sensing.

A. Distribution of the Test Statistic

LRT Detector: From (4) and (8), the test statistic under the null hypothesis is a weighted combination of J independent chi-square random variables with $2M$ degrees of freedom,

$$T = \sum_{j=1}^{J} w_j X_j, \quad w_j = \frac{g_j}{2(1+g_j)}. \tag{30}$$

The weighted sum of chi-square random variables does not have a closed-form cumulative distribution function (cdf). Accurate closed-form approximations have been proposed in the technical literature (see [30] and references therein). In this work, we adopt the Hall-Buckley-Eagleson approximation [29]. This is a moment-matching method that approximates the distribution of T by a gamma distribution with the following cdf

$$F_T(\gamma) \approx F_{\Gamma(K,\theta)}\left(\frac{4k_2}{k_3}(\gamma - k_1) + \frac{8k_2^3}{k_3^2}\right), \tag{31}$$

where k_1, k_2 and k_3 are the first three cumulants of T, given by

$$k_1 = 2M\sum_{j=1}^{J} w_j, \quad k_2 = 4M\sum_{j=1}^{J} w_j^2, \; k_3 = 16M\sum_{j=1}^{J} w_j^3, \tag{32}$$

and the shape and scale parameters of the gamma distribution are $K = 4k_2^3/k_3^2$ and $\theta = 2$, respectively.

EGC Detector: Substituting (4) in (9) the distribution of the EGC test statistic under the null hypothesis is chi-square with $2MJ$ degrees of freedom. Therefore, it only depends on the known parameters M and J.

GLRT Detector: Substituting (4) in (12), after simple algebraic manipulations, the test statistic of the GLRT under the null hypothesis is distributed as follows

$$\sum_{j=1}^{J}\left(\frac{1}{2}X_{\text{j-M}}\right)^{+}, \tag{33}$$

where, as above, $X_j \sim \chi^2_{2M}$. Notice that the distribution is independent of the SNRs. Since it only depends on known parameters, M and J, it can be computed in advance.

EM Detector: Substituting (4) in (29), the test statistic under the null hypothesis has the same form as in the LRT (8), but now the weights are functions of the SNRs estimates at time $n-1$ (i.e., at time n they are fixed and known quantities)

$$w_j = \frac{\hat{g}_{n-1,j}}{2(1+\hat{g}_{n-1,j})}. \tag{34}$$

Therefore, the distribution of the test statistic under the null hypothesis can also be approximated by (31) with the weights given by (34).

B. Decision Thresholds

From (31), the probability of false alarm of the LRT and EM detectors, for a given threshold γ, will be

$$P_{FA}(\gamma) = 1 - F_{\Gamma(K,\theta)}\left(\frac{4k_2}{k_3}(\gamma - k_1) + \frac{8k_2^3}{k_3^2}\right), \tag{35}$$

where the cumulants, given by (32), are computed from the weights in (30) and (34), respectively. Since $P_{FA}(\gamma)$ is monotonically decreasing, the threshold to guarantee a prescribed probability of false alarm can be easily obtained from (35) by using conventional root-finding algorithms like bisection, secant, or Newton's method. Notice that the decision threshold depends on the actual (LRT) or estimated (EM) SNRs through the cumulants in (35). Therefore, it must be computed each time these values change. As it was mentioned above, the distributions of the GLRT and EGC test statistic, under the null hypothesis, only depend on J and M, which are known parameters. Therefore, the thresholds can be calculated and set in advance, regardless of the values of the SNRs at each time.

VI. Simulation Results

A. Experimental Setup

We have considered the following assumptions:

- The CRs measure the signal energy periodically, being T the time elapsed between consecutive measurements. After each measurement, the CRs report the energy values to the FC through the control channels, which are assumed to be error-free. We also assume that the PU state does not change during the sampling intervals when the CRs acquire the M signal samples to estimate the energy level. But it can change between consecutive energy measurements.
- The PU activity, s_n, is modeled as a homogeneous Markov chain with two states: inactive ($s = 0$) and active ($s = 1$). This model has been widely used in the technical literature [39], [40]. According to [40], we assume that the transition probabilities are $\mathrm{P}(s_n = 0|s_{n-1} = 0) = 1 - \alpha_1, \mathrm{P}(s_n = 1|s_{n-1} = 1) = \alpha_1$, where α_1 is the COR. The PU activity model is unknown by the FC, but we assume that it knows the COR.
- We assume that the sensing channels are independent and identically Rayleigh distributed. Therefore, the SNRs at the CRs will be independent and exponentially distributed, with identical mean $\mathbb{E}[g_j] = \bar{g}, \quad j = 1, \ldots, J$. The sensing channels (and therefore the SNRs) are time-varying. The time correlation between the energy measurements is determined by the channels Doppler shift normalized to $1/T$, which is denoted by f_D. We assume that f_D is the same for all sensing channels. In the simulations, we generate time-correlated realizations using the Jakes' model [41] with the corresponding f_D. It is important to remark that the above channel model is just the one we adopt in the simulations by default. Any other model, with a different distribution, could be used, as these distributions are not used in the derivation of the proposed approach.

Unless otherwise indicated we consider the following values for the model parameters: $J = 3$, $M = 32$, $\alpha_1 = 0.5$, $\bar{g} = -3$ dB and $f_D = 2 \cdot 10^{-3}$. They can be realistic values in practical mobile scenarios. The following results show how the detection and estimation performance depends on such parameters.

B. Performance of the EM Estimator

We first study how the estimation performance of the EM algorithm evolves, in stationary and in time-varying scenarios, by means of Monte Carlo simulations. We average the performance of $R = 10^5$ independent runs, each one comprising $N = 200$ energy vectors. Each sequence of energy vectors was obtained from realizations, of length N, of the random processes $\mathbf{g}_n$ and s_n according to the models described above. We consider the mean squared error (MSE) at each time n as a performance metric:

$$\mathrm{MSE}_n = \frac{1}{RJ} \sum_{r=1}^{R} ||\hat{\mathbf{g}}_n^{(r)} - \mathbf{g}_n^{(r)}||^2,$$

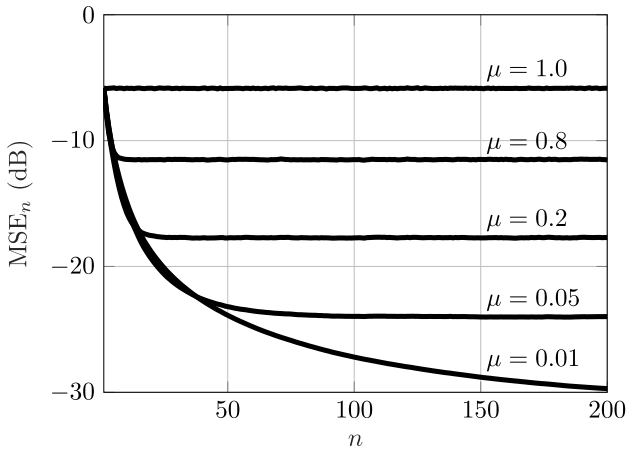

Fig. 1. MSE of the SNR estimates for different values of learning rate in invariant channels ($f_D = 0$).

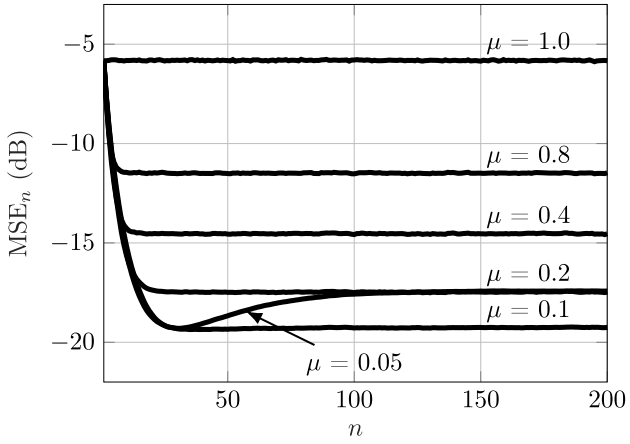

Fig. 2. MSE of the SNR estimates for different values of learning rate in time-variant channels with $f_D = 2 \cdot 10^{-3}$.

where the superscript r denotes the index of each independent run.

Figure 1 shows the MSE curves, for different values of the learning rate, in the stationary case ($f_D = 0$). Therefore, in each run the SNR at each CR is constant, so all energy values are measured with the same SNR. The figure shows that the lower the learning rate the better the MSE. This behavior is explained by the fact that the contribution of the energy observations should not depend on the time the energies were measured. According to (27), this occurs when the forgetting factor tends to zero.

Figure 2 shows the MSE curves when the SNRs are time-varying with $f_D = 2 \cdot 10^{-3}$. For illustration purposes, Figure 3 shows the SNRs realization and the corresponding estimates in one of the R runs. Due to the time correlation, the optimal forgetting factor is no longer zero. The more recent an energy observation is, the more weight it should have in estimating the current SNR (see (25)). These weights are controlled by the forgetting factor, being $\mu \approx 0.1$ the optimal in this case.

To explain the transient MSE for small values of the forgetting factor, as $\mu = 0.05$, we have to resort to (25) and

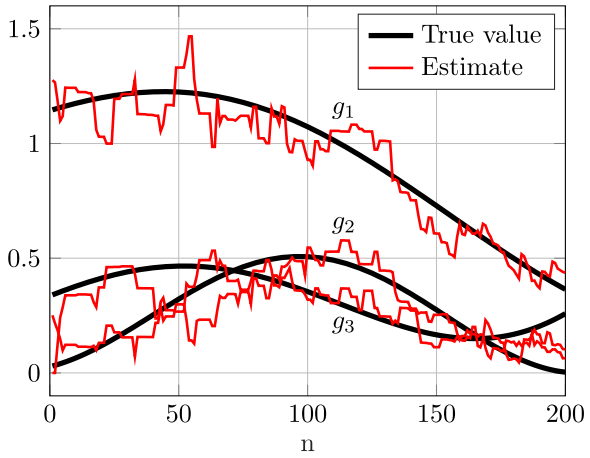

Fig. 3. SNRs and their estimates for $\mu = 0.1$.

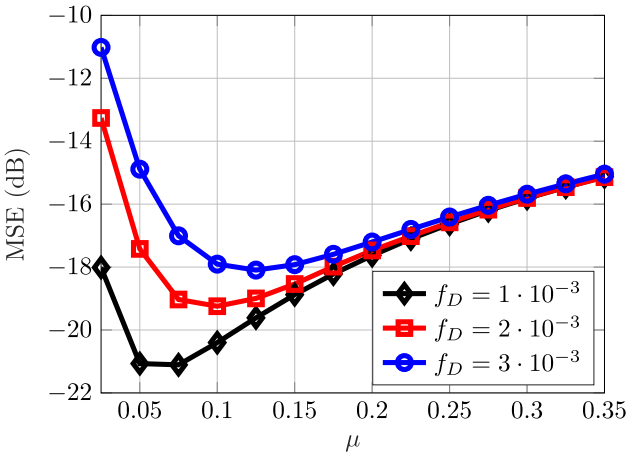

Fig. 4. MSE versus forgetting factor for different values of Doppler shift.

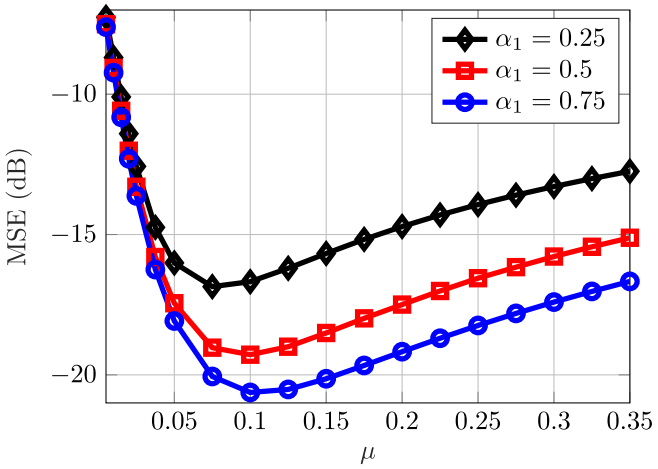

Fig. 5. MSE versus forgetting factor for different values of COR.

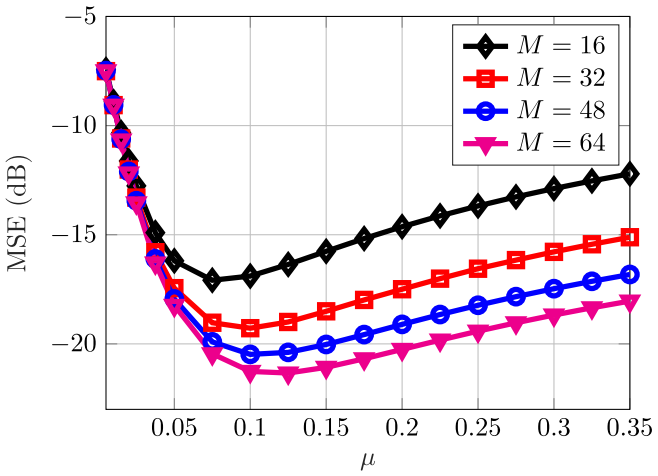

Fig. 6. MSE versus forgetting factor for different values of M.

its asymptotic (27). When μ is small, the first estimates of the SNR (for small n) are very similar (see (25)) and close to (27). The value of f_D determines how many consecutive energy vectors are measured under similar SNRs. Let us denote it as N_D. Then, when $n < N_D$ the energy measurements up to n have been measured under similar SNRs values. In this case, small values of μ are optimal, as Figure 2 shows. But, when $n > N_D$ the last energy vectors are measured under different SNRs values, so small values of μ are no longer optimal.

In the following figures we show the performance of the EM estimator in the stationary regime, that is, when n is large enough so the MSE does not depend on it. In this case, taking advantage of the ergodicity of $\mathbf{g}_n$ and s_n, we consider a single but very long run, $N = 2 \cdot 10^7$, to estimate the MSE. Now, it will be

$$\text{MSE} = \frac{1}{NJ} \sum_{n=1}^{N} ||\hat{\mathbf{g}}_n - \mathbf{g}_n||^2.$$

Figure 4 shows the MSE versus the forgetting factor for different values of normalized Doppler shift. As it is expected, the higher the correlation of the SNR values (lower f_D), the lower is the optimal forgetting factor. Interestingly, the optimal forgetting factor is similar (around $\mu = 0.1$) in the three curves even though the time correlation of the SNRs is quite different.

Figure 5 shows the MSE versus the forgetting factor for different values of COR. As it is expected, performance degrades when α_1 decreases. This is because the less active is the PU, the fewer energy values are available to estimate the primary SNR. It is also observed that the less active is the PU, the higher is the optimal forgetting factor because the energy measurements with primary signals are more sparse in time. In any case, despite this trend, one can observe that the optimal forgetting factor is quite similar (around $\mu = 0.1$) in all cases.

Figure 6 shows the MSE versus the forgetting factor for different numbers of signal samples, M, used to estimate the energy. The higher the M, the more accurate are the energy estimates, and therefore, the better is the MSE. It is also observed that the optimal forgetting factor depends little on M. It is around $\mu = 0.1$ in all cases.

Figure 7 shows the MSE versus the forgetting factor for different number of CRs. The optimum forgetting factor does not depend on the number of CRs. Performance improves slightly as the number of CRs increases. This improvement

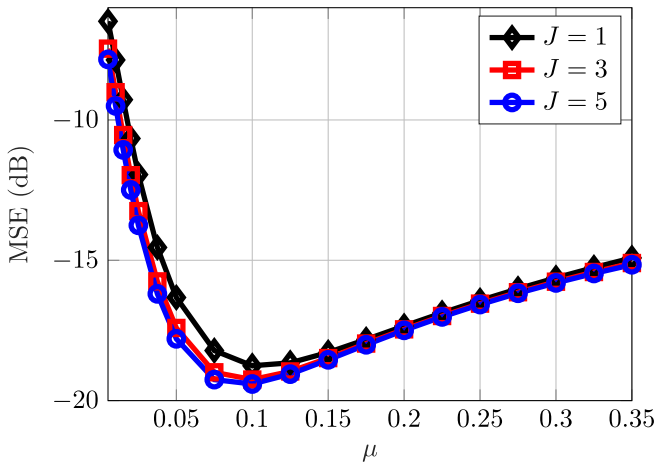

Fig. 7. MSE versus forgetting factor for different number of CRs.

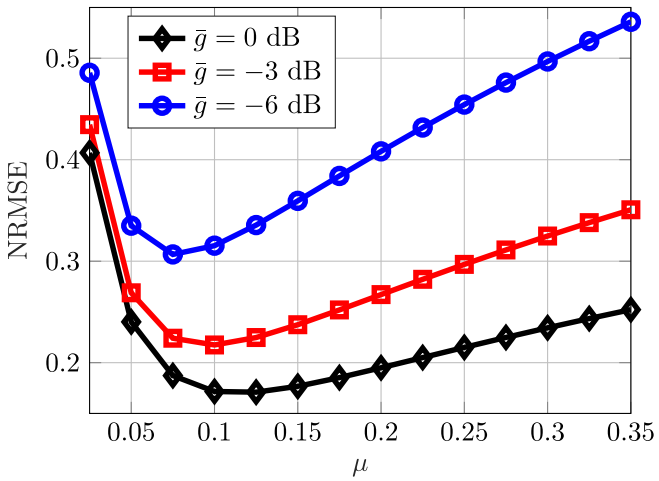

Fig. 8. NRMSE versus forgetting factor for different values of average SNR.

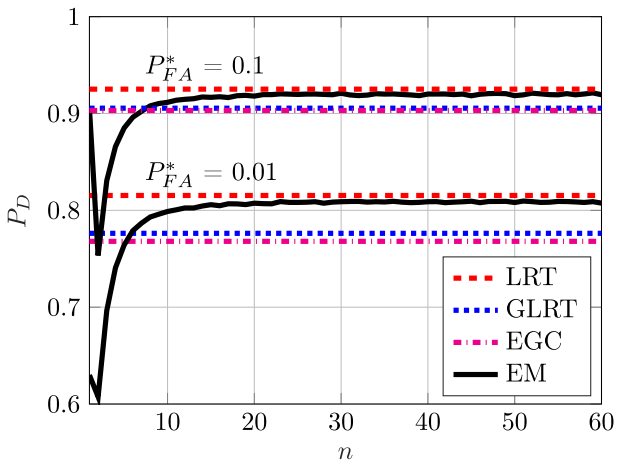

Fig. 9. Transient behavior of the detection probability for different prescribed probabilities of false alarm P^*_{FA}.

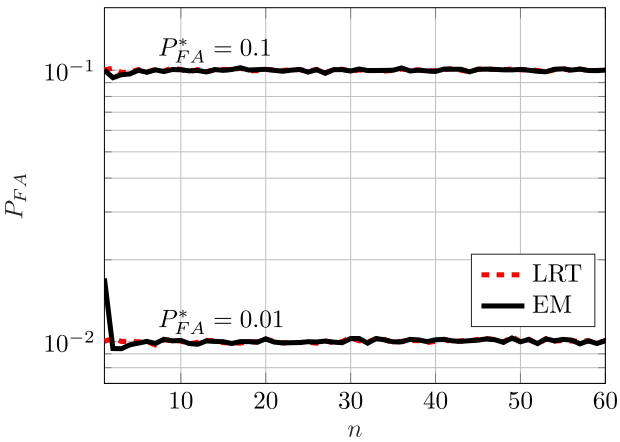

Fig. 10. Transient behavior of the false alarm probabilities.

comes from the E-step (21) because the responsibilities are computed more accurately from more energy measurements. On the other hand, in the M-step (22) there is no benefit from using more CRs. This is because the energy measurements at different CRs are almost independent, so the SNR at a given CR is estimated only from its local energy level.

Figure 8 shows the estimation performance, as a function of the forgetting factor, for different values of average SNR. To compare performance curves with different average SNR we employ the normalized root MSE (NRMSE) as a performance metric, defined as

$$\text{NRMSE} = \frac{1}{\bar{g}}\sqrt{\frac{1}{NJ}\sum_{n=1}^{N}||\hat{\mathbf{g}}_n - \mathbf{g}_n||^2}. \tag{36}$$

As it is expected, the higher the average SNR, the better the performance. The optimal forgetting factor does not change significantly with the average SNR.

Figures 4 to 8 show that $\mu = 0.1$ is a good choice in all cases. It is close to the optimum for a wide range of the parameters' values.

C. Performance of the EM Detector

In this section, we compare the detection performance of the EM detector with the LRT, the one-shot GLRT, and the EGC detectors. For the LRT the SNRs are assumed to be known, so its performance can be considered as an upper bound for the others. The performance metric is the probability of detection, P_D, for a given probability of false alarm, P_{FA}.

First, we study the transient behavior of the EM detector, in time-varying scenarios, by means of Monte Carlo simulations. We average the performance of $R = 10^5$ independent runs, each one comprising $N = 60$ energy vectors. Unless otherwise indicated, the values of the simulation parameters are the ones mentioned in Section VI-A.

Figure 9 shows the detection probability for two values of prescribed probability of false alarm: $P^*_{FA} = \{0.1, 0.01\}$. The forgetting factor is $\mu = 0.1$. It is observed that after $n = 20$ energy observations the detection probabilities reach stationary values. It agrees with the transient estimation behavior shown in Figure 2.

Figure 10 depicts the corresponding curves of probability of false alarm. They show that the moment-matching approximation (35) to set the decision threshold is very good. It is

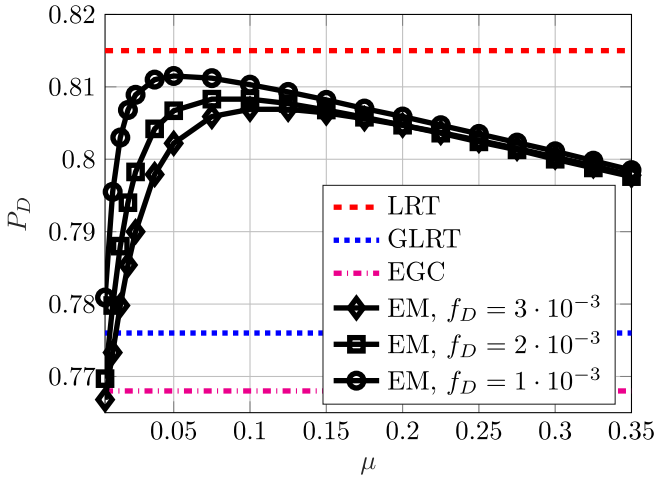

Fig. 11. Detection probability versus forgetting factor for different values of Doppler shift.

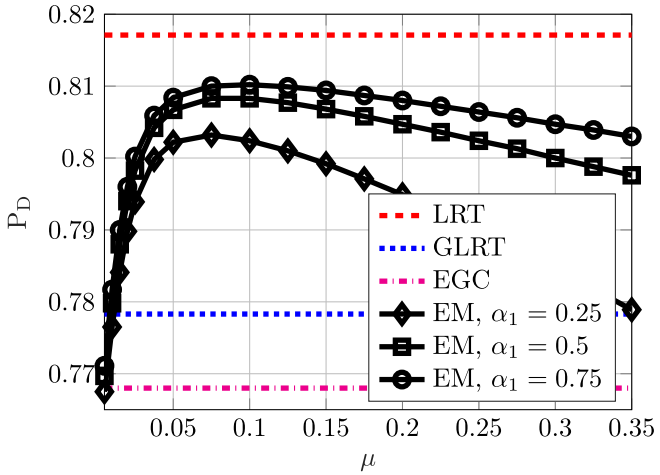

Fig. 12. Detection probability versus forgetting factor for different values of COR.

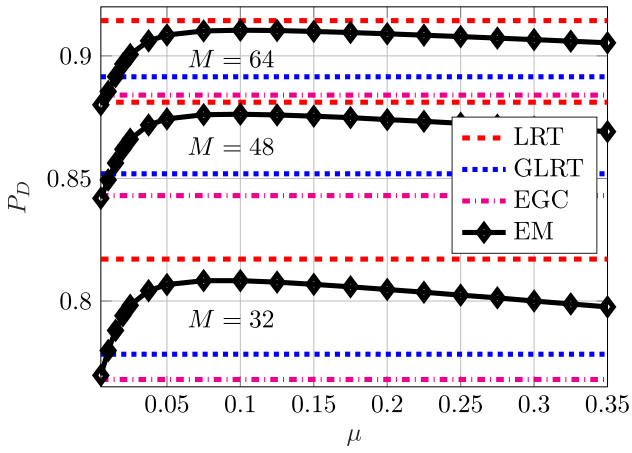

Fig. 13. Detection probability versus forgetting factor for different values of M.

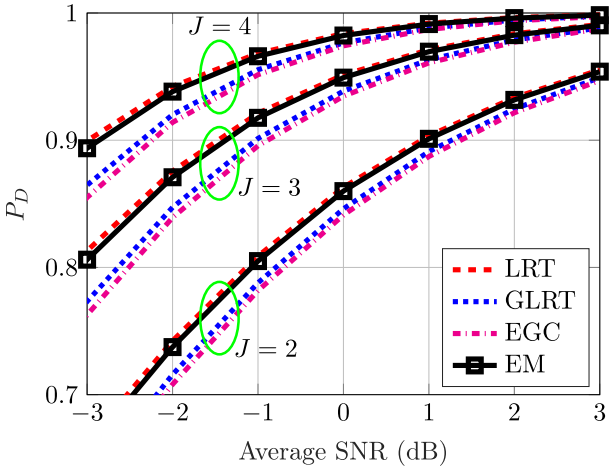

Fig. 14. Detection probability versus average SNR for different number of CRs.

observed that, once the SNRs have been properly estimated, the EM detector threshold is precisely set.

Figures 9 and 10 show an undesirable transient behavior in the first iterations due to the fact that the number of past energy observations is insufficient for a precise estimation of the SNRs (see Figure 2). A simple way to overcome this is to use the GLRT (12) in the early iterations and switch to the EM detector after the number of energy observations is enough for an acceptable SNRs estimation. The figures show that, after a few energy observations, the EM detector outperforms the GLRT, and the decision threshold for the prescribed P_{FA}^* is accurately obtained.

In the following figures we show the performance of the EM detector in the stationary regime, that is, when the number of past energy observations is enough so the detection performance does not depend on it. Again, taking advantage of the ergodicity of the models of $\mathbf{g}_n$ and s_n, we consider a single but very long run of $N = 2 \cdot 10^5$ energy observations to estimate the stationary detection performance. Unless otherwise indicated the prescribed probability of false alarm is $P_{FA}^* = 0.01$.

Figure 11 shows the probability of detection versus μ for different Doppler shifts. As it is expected, the optimal forgetting factor increases slightly when the Doppler shift increases because the energy measurements exhibit less correlation. In any case, it is quite close to $\mu = 0.1$ for a wide range of f_D values. Moreover, in all cases, the EM algorithm shows good detection performance even for μ values much bigger than the optimal one.

Figure 12 shows the detection probability for different values of COR. As it is expected, the detection performance is better for higher values of COR because more energy vectors are observed when the PU is active. As in the previous figure, the optimal μ is close to 0.1 in all cases.

Figure 13 shows the detection probability for different values of M. The probability of detection is quite sensitive to M. A small increment in M leads to significant performance improvement. As in previous figures, the optimal forgetting factor is close to $\mu = 0.1$, and the performance does not degrade significantly for large deviations from it.

Figure 14 shows how the inherent diversity of the cooperative spectrum sensing improves detection performance. It is

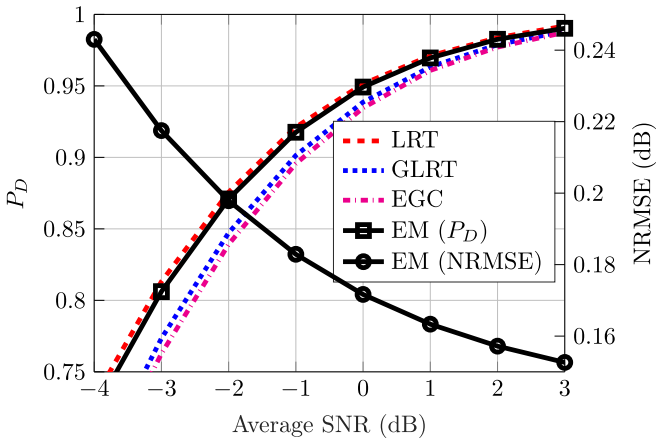

Fig. 15. Detection probability and NRMSE of the EM estimator versus average SNR.

observed that the detection probability is very sensitive to the number of CRs. The forgetting factor was $\mu = 0.1$ in all cases.

Finally, Figure 15 shows the detection probability as a function of the average SNR together with the NRMSE of the EM estimates. The forgetting factor was $\mu = 0.1$ in all cases. As expected, the better the estimation performance, the closer the EM detector is to the LRT. In any case, the estimation performance of the EM algorithm is good enough that the probability of detection hardly deviates from that of the LRT over the entire SNR range.

VII. Conclusion

We have presented a new adaptive algorithm for cooperative spectrum sensing based on the soft fusion of energy measurements of the sensors. The algorithm jointly detects the channel occupancy and estimates the SNR at the energy sensors. We also propose an accurate method to calculate the detection threshold. Due to its adaptive nature, the algorithm is well suited for mobile scenarios where the SNR at the sensors change over time. Numerical simulations show that the algorithm can efficiently track the SNRs, so its detection performance is close to the likelihood ratio test in realistic conditions.

Appendix A
ML Estimation of the SNR

The ML estimate of g_j, from e_j, under H_1 is

$$\hat{g}_j = \underset{g_j \geq 0}{\operatorname{argmax}} \; f(e_j | s = 1, g_j)$$

Considering (5) and taking logarithms,

$$\hat{g}_j = \underset{g_j \geq 0}{\operatorname{argmin}} \; M \log(1 + g_j) + \frac{e_j}{1 + g_j} \tag{37}$$

This is a single-variable optimization problem with an inequality constraint. The Karush-Kuhn-Tucker (KKT) conditions are

$$M(1 + g_j) - e_j - \lambda(1 + g_j)^2 = 0, \quad \lambda \, g_j = 0, \quad \lambda \geq 0, \quad -g_j \leq 0,$$

where λ is the Lagrange multiplier.

- If the constraint were inactive, $g_j > 0 \Rightarrow \lambda = 0$ Then, the KKT conditions reduce to

  $$M(1 + g_j) - e_j = 0, \qquad g_j > 0$$

  From the equality, we obtain $g_j = \frac{e_j}{M} - 1$, and the inequality requires $e_j > M$.
- If the constraint were active, $g_j = 0$. Then, the KKT conditions reduce to

  $$M - e_j - \lambda = 0, \qquad \lambda \geq 0.$$

  From the equality, we have $\lambda = M - e_j$, and the inequality requires $e_j \leq M$

The results from the two cases can be compactly written as

$$\hat{g}_j = \left(\frac{e_j}{M} - 1 \right)^+.$$

Appendix B
Derivation of the One-Shot GLRT

From (11), there are two possible cases,

- if $e_j \leq M \Rightarrow \hat{g}_j = 0$, then, the jth term in the GLR (10) will be $e_j \frac{\hat{g}_j}{1+\hat{g}_j} = 0$.
- if $e_j > M \Rightarrow \hat{g}_j = e_j/M - 1$, then, the jth term in the GLR (10) will be

$$e_j \frac{\hat{g}_j}{1 + \hat{g}_j} = e_j \frac{e_j/M - 1}{e_j/M} = e_j \frac{e_j - M}{e_j} = e_j - M.$$

Finally, the above expressions can be written compactly as follows

$$e_j \frac{\hat{g}_j}{1 + \hat{g}_j} = (e_j - M)^+. \tag{38}$$

Appendix C
Complete-Data Likelihood in Exponential Family Form

Given $\mathbf{e}$ and s, the complete-data likelihood can be written as follows

$$L_c(\mathbf{g}) = [\alpha_0 \; f(\mathbf{e}|s = 0)]^{1-s} \; [\alpha_1 \; f(\mathbf{e}|s = 1, \mathbf{g})]^s.$$

Considering (5) and (6), it becomes

$$\begin{aligned} L_c(\mathbf{g}) &= [\alpha_0 \; f(\mathbf{e}|s = 0)]^{1-s} \left[\alpha_1 \prod_{j=1}^{J} \frac{e_j^{M-1}}{\Gamma(M)} \right]^s \\ &\quad \left[\prod_{j=1}^{J} (1 + g_j)^{-M} \exp\left(\frac{-e_j}{1 + g_j} \right) \right]^s \\ &= [\alpha_0 \; f(\mathbf{e}|s = 0)]^{1-s} \left[\alpha_1 \prod_{j=1}^{J} \frac{e_j^{M-1}}{\Gamma(M)} \right]^s \\ &\quad \exp\left(-s \sum_{j=1}^{J} M \log(1 + g_j) + \frac{e_j}{1 + g_j} \right). \end{aligned}$$

Then, denoting

$$h(\mathbf{e},s) = [\alpha_0\ f(\mathbf{e}|s=0)]^{1-s}\ \left[\alpha_1 \prod_{j=1}^{J} \frac{e_j^{M-1}}{\Gamma(M)}\right]^{s},$$

$$\boldsymbol{\eta}(\mathbf{g}) = -\begin{pmatrix} M\sum_{j=1}^{J}\log(1+g_j) \\ (1+g_1)^{-1} \\ \vdots \\ (1+g_J)^{-1} \end{pmatrix}, \quad \boldsymbol{\Phi}(\mathbf{e},s) = \begin{pmatrix} s \\ e_1\ s \\ \vdots \\ e_J s \end{pmatrix}, \tag{39}$$

the complete-data likelihood can be written in exponential family form, i.e.,

$$L_c(\mathbf{g}) = h(\mathbf{e},s)\ \exp\left[\boldsymbol{\eta}(\mathbf{g})^T \boldsymbol{\Phi}(\mathbf{e},s)\right].$$

APPENDIX D
E-STEP: CONDITIONAL EXPECTATION OF THE SUFFICIENT STATISTIC

Considering (17), the conditional expectation of the sufficient statistic at time n will be

$$\mathbb{E}\left[\boldsymbol{\Phi}(\mathbf{e}_n, s_n)|\mathbf{e}_n, \hat{\mathbf{g}}_{n-1}\right] = \ \tilde{s}_n \begin{pmatrix} 1 \\ \mathbf{e}_n \end{pmatrix},$$

where the responsibility is given by

$$\tilde{s}_n = \mathbb{E}\left[s_n|\mathbf{e}_n, \hat{\mathbf{g}}_{n-1}\right] = P(s_n = 1|\mathbf{e}_n, \hat{\mathbf{g}}_{n-1}),$$

which is the probability that the PU was active when $\mathbf{e}_n$ was observed, conditioned on the previous SNR estimate $\hat{\mathbf{g}}_{n-1}$.

Applying the Bayes' theorem, it becomes

$$\begin{aligned}\tilde{s}_n &= \frac{f(\mathbf{e}_n|s_n=1,\hat{\mathbf{g}}_{n-1})\ f(s_n=1)}{f(\mathbf{e}_n|\hat{\mathbf{g}}_{n-1})} \\ &= \frac{\alpha_1\ f(\mathbf{e}_n|s_n=1|\hat{\mathbf{g}}_{n-1})}{\alpha_0\ f(\mathbf{e}_n|s_n=0) + \alpha_1\ f(\mathbf{e}_n|s_n=1,\hat{\mathbf{g}}_{n-1})} \\ &= \left[1 + \frac{\alpha_0\ f(\mathbf{e}_n|s_n=0)}{\alpha_1\ f(\mathbf{e}_n|s_n=1,\hat{\mathbf{g}}_{n-1})}\right]^{-1}.\end{aligned}$$

Considering the conditional pdf of the energy vectors, given by (6) and (5), the responsibility can be written as

$$\tilde{s}_n = \left[1 + \frac{\alpha_0}{\alpha_1}\prod_{j=1}^{J}(1+\hat{g}_{n-1,j})^M \exp\left(-\frac{e_{n,j}\ \hat{g}_{n-1,j}}{1+\hat{g}_{n-1,j}}\right)\right]^{-1}.$$

Then, (19) can be expressed as follows

$$\boldsymbol{\phi}_n = \left[\ b_n\ \mathbf{a}_n^T\ \right]^T,$$

where

$$b_n = (1-\mu)\ b_{n-1} + \mu\ \tilde{s}_n, \quad \boldsymbol{a}_n = (1-\mu)\ \boldsymbol{a}_{n-1} + \mu\ \tilde{s}_n\ \mathbf{e}_n.$$

APPENDIX E
M-STEP: ESTIMATION OF THE INSTANTANEOUS PRIMARY SNR

The estimate of the SNR vector at time n is given by (15). Then, considering the parameters function in (17), the M-step becomes

$$\begin{aligned}\hat{\mathbf{g}}_n &= \underset{\mathbf{g}\geq\mathbf{0}}{\operatorname{argmax}}\ -b_n\sum_{j=1}^{J} M\log(1+g_j) - \sum_{j=1}^{J}\frac{a_{n,j}}{1+g_j} \\ &= \underset{\mathbf{g}\geq\mathbf{0}}{\operatorname{argmin}}\ \sum_{j=1}^{J} b_n M\log(1+g_j) + \frac{a_{n,j}}{1+g_j}.\end{aligned}$$

Since the terms of the objective function are decoupled, the optimization problem can be divided into J decoupled constrained optimization problems of the form

$$\hat{g}_{n,j} = \underset{g_j\geq 0}{\operatorname{argmin}}\ Mb_n\log(1+g_j) + \frac{a_{n,j}}{1+g_j}.$$

Notice that it has the same form than (37) changing Mb_n and $a_{n,j}$ by M and e_j. Therefore, the instantaneous SNRs estimates will be

$$\hat{g}_{n,j} = \left(\frac{a_{n,j}}{M\ b_n} - 1\right)^+.$$

REFERENCES

[1] I. F. Akyildiz, B. F. Lo, and R. Balakrishnan, "Cooperative spectrum sensing in cognitive radio networks: A survey," *Phys. Commun.*, vol. 4, no. 1, pp. 40–62, Mar. 2011.

[2] Y. Zeng, Y.-C. Liang, A. T. Hoang, and R. Zhang, "A review on spectrum sensing for cognitive radio: Challenges and solutions," *EURASIP J. Adv. Signal Process.*, vol. 2010, no. 1, pp. 1–15, Jan. 2010.

[3] Q. Zhi, C. Shuguang, H. Poor, and A. Sayed, "Collaborative wideband sensing for cognitive radios," *IEEE Signal Process. Mag.*, vol. 25, no. 6, pp. 60–73, Nov. 2008.

[4] E. Axell, G. Leus, E. Larsson, and H. Poor, "Spectrum sensing for cognitive radio: State-of-the-art and recent advances," *IEEE Signal Process. Mag.*, vol. 29, no. 3, pp. 101–116, May 2012.

[5] K. M. Thilina, K. W. Choi, N. Saquib, and E. Hossain, "Machine learning techniques for cooperative spectrum sensing in cognitive radio networks," *IEEE J. Sel. Areas Commun.*, vol. 31, no. 11, pp. 2209–2221, Nov. 2013.

[6] D. Hamza, S. Aïssa, and G. Aniba, "Equal gain combining for cooperative spectrum sensing in cognitive radio networks," *IEEE Trans. Wireless Commun.*, vol. 13, no. 8, pp. 4334–4345, Aug. 2014.

[7] J. Ma, G. Zhao, and Y. Li, "Soft combination and detection for cooperative spectrum sensing in cognitive radio networks," *IEEE Trans. Wireless Commun.*, vol. 7, no. 11, pp. 4502–4507, Nov. 2008.

[8] P. B. Gohain, S. Chaudhari, and V. Koivunen, "Cooperative energy detection with heterogeneous sensors under noise uncertainty: SNR wall and use of evidence theory," *IEEE Trans. Cogn. Commun. Netw.*, vol. 4, no. 3, pp. 473–485, Sep. 2018.

[9] M. Naderipour, A. Taherpour, A. Taherpour, and S. Gazor, "Design of optimal non-uniform quantizer in imperfect noisy reporting channels for collaborative spectrum sensing," *IEEE Trans. Veh. Technol.*, vol. 69, no. 11, pp. 12870–12882, Nov. 2020.

[10] Z. Wang and W. Zhang, "Exploiting multiuser diversity with 1-bit feedback for spectrum sharing," *IEEE Trans. Commun.*, vol. 62, no. 1, pp. 29–40, Jan. 2014.

[11] J. So, "Cooperative spectrum sensing for cognitive radio networks with limited reporting," *KSII Trans. Internet Inf. Syst.*, vol. 9, no. 8, pp. 2755–2773, 2015.

[12] H. V. Poor, *An Introduction to Signal Detection and Estimation*. New York, NY, USA: Springer-Verlag, 1994.

[13] S. M. Kay, *Fundamentals of Statistical Signal Processing: Detection Theory* (Signal Processing Series). Upper Saddle River, NJ, USA: Prentice-Hall, 1998.

[14] Z. Quan, S. Cui, and A. H. Sayed, "Optimal linear cooperation for spectrum sensing in cognitive radio networks," *IEEE J. Sel. Topics Signal Process.*, vol. 2, no. 1, pp. 28–40, Feb. 2008.
[15] J. Tong, M. Jin, Q. Guo, and Y. Li, "Cooperative spectrum sensing: A blind and soft fusion detector," *IEEE Trans. Wireless Commun.*, vol. 17, no. 4, pp. 2726–2737, Apr. 2018.
[16] H. Guo, W. Jiang, and W. Luo, "Linear soft combination for cooperative spectrum sensing in cognitive radio networks," *IEEE Commun. Lett.*, vol. 21, no. 7, pp. 1573–1576, Jul. 2017.
[17] S. Zarrin and T. J. Lim, "Cooperative spectrum sensing in cognitive radios with incomplete likelihood functions," *IEEE Trans. Signal Process.*, vol. 58, no. 6, pp. 3272–3281, Jun. 2010.
[18] J. Perez, I. Santamaria, and J. Via, "Adaptive EM-based algorithm for cooperative spectrum sensing in mobile environments," in *Proc. IEEE Stat. Signal Process. Workshop (SSP)*, Freiburg, Germany, Jun. 2018, pp. 732–736.
[19] Q. Zou, S. Zheng, and A. H. Sayed, "Cooperative sensing via sequential detection," *IEEE Trans. Signal Process.*, vol. 58, no. 12, pp. 6266–6283, Dec. 2010.
[20] A. Wald, *Sequential Analysis*. New York, NY, USA: Wiley, 1947.
[21] S. Chaudhari, V. Koivunen, and H. V. Poor, "Autocorrelation-based decentralized sequential detection of OFDM signals in cognitive radios," *IEEE Trans. Signal Process.*, vol. 57, no. 7, pp. 2690–2699, Jul. 2009.
[22] J. Manco-Vásquez, M. Lázaro-Gredilla, D. Ramírez, J. Vía, and I. Santamaría, "A Bayesian approach for adaptive multiantenna sensing in cognitive radio networks," *Signal Process.*, vol. 96, pp. 228–240, Mar. 2014.
[23] S. K. Sharma, S. Chatzinotas, and B. Ottersten, "Eigenvalue-based sensing and SNR estimation for cognitive radio in presence of noise correlation," *IEEE Trans. Veh. Technol.*, vol. 62, no. 8, pp. 3671–3684, Oct. 2013.
[24] C. M. Bishop, *Pattern Recognition and Machine Learning*. New York, NY, USA: Springer, 2006.
[25] K. P. Murphy, *Machine Learning: A Probabilistic Perspective*. Cambridge, MA, USA: MIT Press, 2012.
[26] A. Same, C. Ambroise, and G. Govaert, "An online classification em algorithm based on the mixture model," *Statist. Comput.*, vol. 17, pp. 209–218, Jun. 2007.
[27] M. Sato and S. Ishii, "On-line EM algorithm for the normalized Gaussian network," *Neural Comput.*, vol. 12, pp. 407–432, Mar. 2000.
[28] O. Cappe and E. Moulines, "On-line expectation–maximization algorithm for latent data models," *J. Roy. Stat. Soc. B, Stat. Methodol.*, vol. 71, no. 3, pp. 593–613, Jun. 2009.
[29] M. J. Buckley and G. K. Eagleson, "An approximation to the distribution of quadratic forms in normal random variables," *Austral. J. Statist.*, vol. 30A, no. 1, pp. 150–159, May 1988.
[30] D. A. Bodenham and N. M. Adams, "A comparison of efficient approximations for a weighted sum of chi-squared random variables," *Statist. Comput.*, vol. 26, pp. 917–928, Jul. 2016.
[31] K. W. Choi, E. Hossain, and D. I. Kim, "Cooperative spectrum sensing under a random geometric primary user network model," *IEEE Trans. Wireless Commun.*, vol. 10, no. 6, pp. 1932–1944, Jun. 2011.
[32] J. A. Gubner, *Probability and Random Processes for Electrical and Computer Engineers*. Cambridge, U.K.: Cambridge Univ. Press, 2006.
[33] J. J. Lehtomaki, R. Vuohtoniemi, and K. Umebayashi, "On the measurement of duty cycle and channel occupancy rate," *IEEE J. Sel. Areas Commun.*, vol. 31, no. 11, pp. 2555–2565, Nov. 2013.
[34] W. Gabran, C.-H. Liu, P. Pawelczak, and D. Cabric, "Primary user traffic estimation for dynamic spectrum access," *IEEE J. Sel. Areas Commun.*, vol. 31, no. 3, pp. 544–558, Mar. 2013.
[35] J. J. Lehtomaki, M. Lopez-Benitez, K. Umebayashi, and M. Juntti, "Improved channel occupancy rate estimation," *IEEE Trans. Commun.*, vol. 63, no. 3, pp. 643–654, Mar. 2015.
[36] M. Lopez-Benitez, A. Al-Tahmeesschi, D. K. Patel, J. J. Lehtomaki, and K. Umebayashi, "Estimation of primary channel activity statistics in cognitive radio based on periodic spectrum sensing observations," *IEEE Trans. Wireless Commun.*, vol. 18, no. 2, pp. 983–996, Feb. 2019.
[37] O. H. Toma, M. Lopez-Benitez, D. K. Patel, and K. Umebayashi, "Estimation of primary channel activity statistics in cognitive radio based on imperfect spectrum sensing," *IEEE Trans. Commun.*, vol. 68, no. 4, pp. 2016–2031, Apr. 2020.
[38] A. P. Dempster, N. M. Laird, and D. B. Rubin, "Maximum likelihood for incomplete data via the EM algorithm," *J. Roy. Statist. Soc. B, Methodol.*, vol. 39, no. 1, pp. 1–38, 1977.
[39] M. Wellens, J. Riihijärvi, and P. Mähönen, "Empirical time and frequency domain models of spectrum use," *Phys. Commun.*, vol. 2, no. 1, pp. 10–32, Mar. 2009.
[40] M. Lopez-Benitez, "Spectrum usage models for the analysis, design and simulation of cognitive radio networks," M.S. thesis, Dept. de Teoria del Senyal i Comunicacions, Univ. Politecnica de Catalunya, Barcelona, Spain, 2001.
[41] T. S. Rappaport, *Wireless Communications*. Upper Saddle River, NJ, USA: Prentice-Hall, 2002.

Jesus Perez received the degree in physics from the University of Cantabria, Spain, and the Ph.D. degree in physics from the University of Cantabria. In 1989, he was with the Radiocommunication and Signal Processing Department, Polytechnic University of Madrid. From 1990 to 1998, he was with the Electronics Department, University of Cantabria. In 1998, he joined the University of Alcalá, where he became an Associate Professor. From 2000 to 2003, he was with T.T.I. Norte. From 2003 to 2007, he was with the Department of Communications Engineering, University of Cantabria, where he is currently an Associate Professor. He has been a Visiting Researcher with the School of Electrical Engineering and Computer Science, Oregon State University. His current research interests include signal processing, machine learning, and communications. He has been involved in several national and international research projects on these topics.

Javier Via received the Telecommunication Engineer degree from the University of Cantabria, Spain, in 2002, and the Ph.D. degree in electrical engineering from the University of Cantabria in 2007. In 2002, he joined the Department of Communications Engineering, University of Cantabria, where he is currently an Associate Professor. He has spent visiting periods at the Smart Antennas Research Group, Stanford University; the Department of Electronics and Computer Engineering, The Hong Kong University of Science and Technology; and the State University of New York at Buffalo. He has actively participated in several European and Spanish research projects. His current research interest includes the application of signal processing techniques in finance.

Luis Vielva was born in Santander, Spain, in 1966. He received the Licenciado degree in physics and the Ph.D. degree in physics from the University of Cantabria, Spain, in 1989 and 1997, respectively, and the degree in mathematics from UNED, Spain, in 2014. In 1989, he joined the Departamento de Ingeniería de Comunicaciones, Universidad de Cantabria, where he is currently an Associate Professor. His current research interests include signal processing, machine learning, and bioinformatics.

David Ramírez (Senior Member, IEEE) received the Telecommunication Engineer degree from the Universidad de Cantabria, Spain, in 2006, and the Ph.D. degree in electrical engineering from the Universidad de Cantabria in 2011. From 2006 to 2011, he was with the Communications Engineering Department, University of Cantabria. In 2011, he joined as a Research Associate with the University of Paderborn, Germany, and later on, he became an Assistant Professor (Akademischer Rat). He is currently an Associate Professor with the Universidad Carlos III de Madrid. He has been a Visiting Researcher with The University of Newcastle, Australia, and University College London. His current research interests include signal processing for wireless communications, statistical signal processing, change-point management, and signal processing over graphs. He has been involved in several national and international research projects on these topics. He is a member of the IEEE Technical Committee on Signal Processing Theory and Methods. He was a recipient of the 2012 IEEE Signal Processing Society Young Author Best Paper Award and the 2013 Extraordinary Ph.D. Award of the University of Cantabria. He was the Publications Chair of the 2018 IEEE Workshop on Statistical Signal Processing. Moreover, he also serves as an Associate Editor for IEEE TRANSACTIONS ON SIGNAL PROCESSING.